Pre-Procedural Imaging of Aortic Root Orientation and Dimensions

Comparison Between X-Ray Angiographic Planar Imaging and 3-Dimensional Multidetector Row Computed Tomography

Vikram Kurra, MD,*† Samir R. Kapadia, MD,* E. Murat Tuzcu, MD,*
Sandra S. Halliburton, PHD,*† Lars Svensson, MD,* Eric E. Roselli, MD,*
Paul Schoenhagen, MD*†

Cleveland, Ohio

Objectives We sought to examine whether contrast-enhanced multidetector row computed tomography (MDCT) allows prediction of X-ray angiographic planes for the root angiogram in the context of transcatheter aortic valve implantation.

Background Understanding of aortic root orientation relative to the body axis is critical for precise positioning of the stent/valve during transcatheter aortic valve implantation.

Methods Forty patients with severe aortic stenosis underwent conventional X-ray angiography and contrast-enhanced MDCT of the aortic root. Oblique MDCT images of the aortic root, corresponding to X-ray angiographic left anterior oblique (LA)/right anterior oblique (RAO) projections, were created. The cranial/caudal angulation was compared between angiographic and reformatted MDCT images. In addition, root diameter measurements were compared.

Results The cranial angulation in the LAO X-ray angiograms (mean LAO: 39 ± 8, n = 38) and matched MDCT images were not significantly different (cranial: 25 ± 7 vs. 23 ± 8; p = 0.214). There was a small but significant difference between the caudal angulation in the RAO angiogram (mean RAO: 25 ± 5, n = 40) and matched CT images (caudal: 21 ± 9 vs. 29 ± 10; p = 0.002). The annulus diameter in the LAO projection was not significantly different between X-ray angiography and contrast-enhanced MDCT (2.3 ± 0.3 vs. 2.4 ± 0.3; p = 0.052), whereas there was a small but significant difference in the annulus diameter in RAO projections between angiography and MDCT (2.4 ± 0.3 vs. 2.2 ± 0.3; p = 0.029).

Conclusions Pre-procedural contrast-enhanced MDCT imaging of the aortic root allows prediction of X-ray angiographic planes and contributes to planning of the transcatheter aortic valve implantation. (J Am Coll Cardiol Intv 2010;3:105–13) © 2010 by the American College of Cardiology Foundation

Pre-procedural assessment of the aortic root for transcatheter aortic valve implantation (TAVI) requires detailed internal measurements but also understanding of the orientation of the root relative to the body axis (1,2). Currently, root orientation is determined by repeated X-ray aortograms in 1 or preferably 2 orthogonal planes before the procedure (Fig. 1). The careful determination of optimal angiographic planes is critical for precise positioning of the stent/valve along the centerline of the aortic root. Ideally this task should be accomplished with limited contrast load.

More recently, several groups have described the use of contrast-enhanced multidetector row computed tomography (MDCT) of the aortic root for procedural planning (3–7). In addition to providing precise measurement, these 3-dimensional (3D) image sets allow the description of the root and aortic valve plane in relation to the body axis. However, comparisons between X-ray angiographic planes and CT reformations for root orientation have not been described (Fig. 2).

We hypothesized that contrast-enhanced MDCT allows prediction of angiographic planes for the root X-ray angiogram, perpendicular to the valve plane.

Figure 1. Conventional Root Angiogram

The current standard root assessment in the context of transcatheter aortic valve insertion is based on the identification of root angiograms before the procedure. In this X-ray angiogram of the aortic root, the valve plane, and the sinuses of Valsalva are illustrated. LCC = left coronary cusp; NCC = noncoronary cusp; RCC = right coronary cusp.

Abbreviations and Acronyms

3D = 3-dimensional

LAO = left anterior oblique

MDCT = multidetector row computed tomography
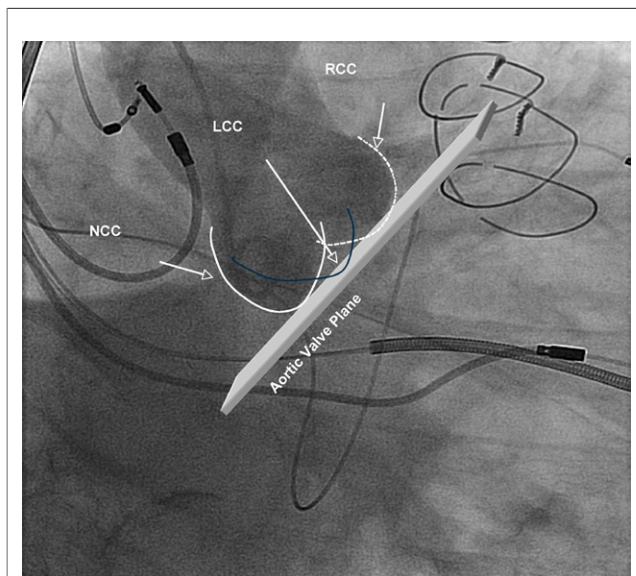
RAO = right anterior oblique

TAVI = transcatheter aortic valve insertion

Methods

Patient population. We prospectively collected contrast-enhanced MDCT and X-ray angiographic data from patients with severe aortic stenosis, undergoing clinical evaluation for percutaneous aortic valve implantation. These patients had a dedicated contrast-enhanced MDCT of the aortic root and conventional coronary angiography with root angiograms performed as part of the pre-procedural evaluation (5,8,9). We screened data from 46 consecutive patients. After excluding 6 cases due to poor MDCT image quality, we included 40 cases for analysis. Use of the data was approved by the local institutional review board with waiver of individual consent.

Contrast-enhanced MDCT acquisition. Patients were scanned on a dual-source MDCT scanner (Definition, Siemens Healthcare, Erlangen, Germany), following administration of 80 to 100 ml of a nonionic, iodinated contrast agent (Ultravist 370, Bayer Healthcare, Berlin, Germany) at 4 to 5 ml/s followed by 30 to 50 ml of normal saline at the same rate. A contrast bolus monitoring technique (10) using a region of interest in the ascending aorta was used to determine the scan delay time. Once the desired attenuation was reached, scanning was initiated in the craniocaudal direction during a single inspiratory breath-hold. Patients were scanned from the level of the carina to the mid-left ventricle. Spiral data were acquired with retrospective electrocardiogram-gating using the following parameters: gantry rotation time = 330 ms; beam collimation = 32 × 0.6 mm; peak tube voltage = 120 kVp; tube current-time product per rotation = 250 to 410 mAs/rot; and beam pitch = 0.2 to 0.5 (depending on heart rate). Electrocardiogram-based tube current modulation was employed for all patients with a reduction in tube current by 80% during systolic phases. Images were reconstructed during 10 to 14 phases of the cardiac cycle depending on patient heart rate with temporal resolution of 83 ms and reconstructed slice thickness of 0.75 mm.

MDCT data analysis. Images were analyzed by consensus of 2 investigators on a dedicated imaging workstation (Leonardo, Siemens Healthcare) using manufacturer software (Circulation and InSpace).

PLANE ORIENTATION. Using an end-diastolic (typically 75% RR-interval) set of axial images, we reformatted the images to a double-oblique view of the sinuses of Valsalva perpendicular to the centerline of the aortic root. In this reformatted image, we centered the cross-hair of the 2 orthogonal locked cut-planes at the coaptation point of the aortic valve leaflets (Fig. 3). We then rotated these planes around the center and observed the resulting oblique sagittal images (Fig. 3). These images corresponded to X-ray angiographic images and the angiographic projection (left anterior oblique [LAO]/right anterior oblique [RAO] and cranial/caudal) is part of the displayed image. We saved 2 sets of these oblique sagittal images, corresponding to the
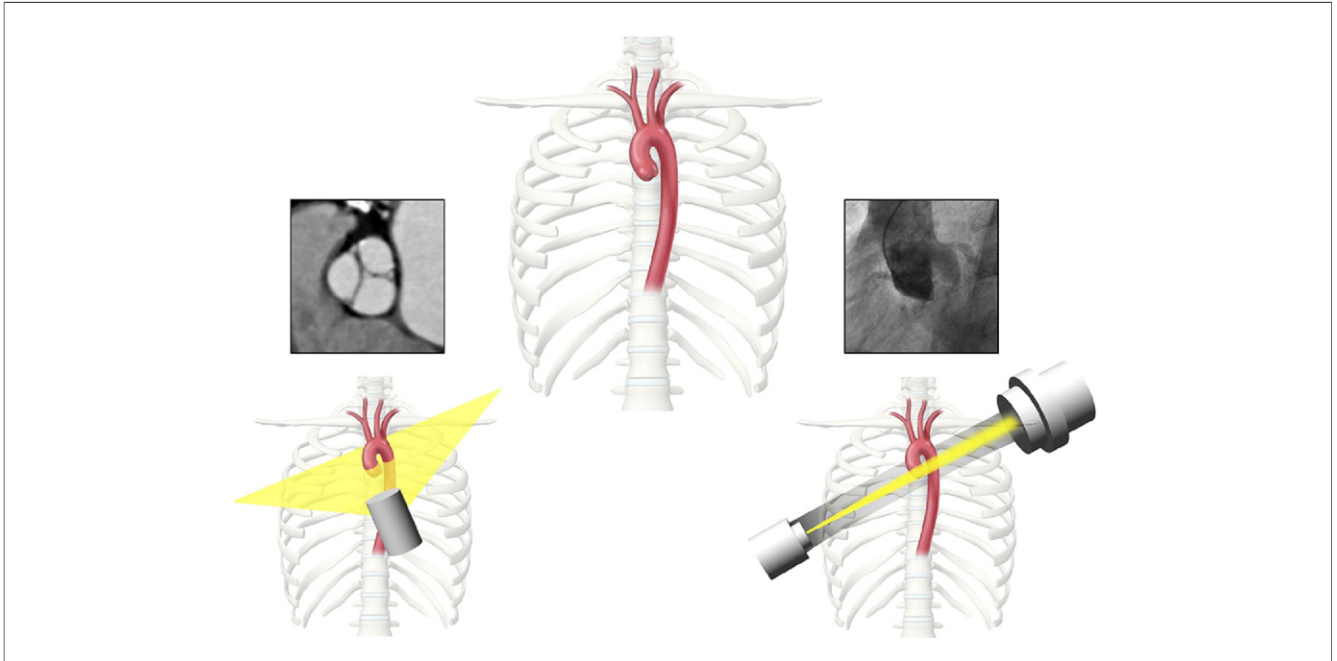
Figure 2. Tomographic and Angiographic Imaging of the Aortic Root

This figure illustrates the different imaging approaches of **(left)** tomographic modalities (cross-sectional images of the valve plane) and **(right)** angiography (orthogonal projection of the aortic root).
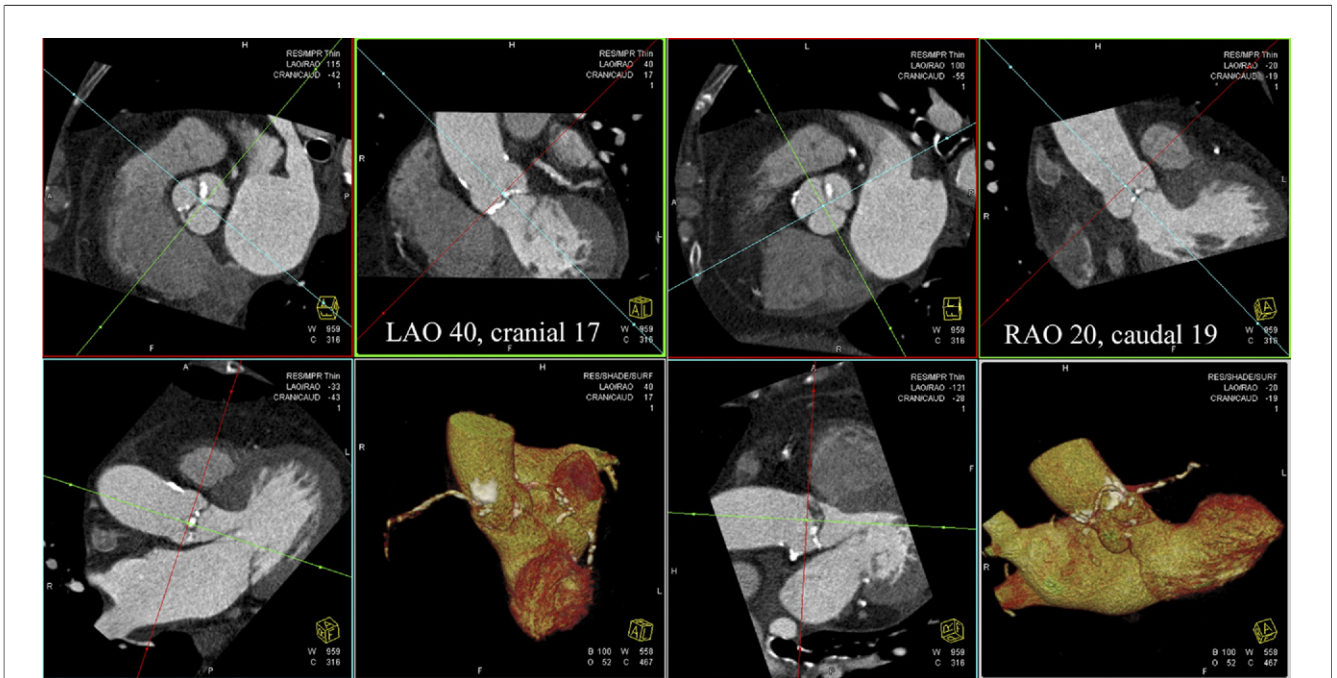
Figure 3. Computed Tomography Images in Specified Angiographic Projections

Reformation of computed tomography images, corresponding to the angiographic left anterior oblique (LAO) and right anterior oblique (RAO) projections. The **upper right panel in each half** corresponds to the final root angiogram in the LAO and RAO projection. The value for the LAO/RAO and cranial/caudal projection is displayed on the screen.

LAO 40 and RAO 20 angiographic projection, and noted the cranial/caudal angulation for these 2 planes. These data were obtained before the diagnostic conventional cardiac catheterization and were available to the angiographic operator at the time of the procedure.

Following the diagnostic X-ray angiographic procedure, during which dedicated root angiograms were obtained, the 2 MDCT investigators, blinded to the full angiographic data, were provided only with the LAO and RAO planes of the final X-ray root angiogram. Using the same method just described, we reformatted corresponding MDCT images and noted the cranial/caudal angulation.

ANNULUS MEASUREMENTS. Two approaches for annulus measurements were used. In the first approach, a cross-sectional MDCT image of the aortic root perpendicular to the centerline at the level of the aortic annulus (defined at the lowest hinge point of the aortic valve leaflets = virtual basal plane) was created and the minimal and maximal annulus diameter measured (Fig. 4). An average diameter was calculated from the minimal and maximal diameters. These measurements were made from a systolic reconstruction (typically 20% to 30% RR-interval).

In the second approach, oblique sagittal reformatted MDCT images of the root were created matching the LAO/RAO projections of the X-ray root angiogram, and the annulus diameter was measured in analogy to the X-ray angiographic measurements (described in the next section) (Fig. 5). Specifically, the annulus was measured at the lowest level of the valve hinge point. In addition, the sinus of Valsalva was measured as the largest diameter of the bulging sinuses, and the sinotubular junction at the junction of the sinuses and tubular portion of the ascending aorta. The MDCT measurements were made in areas of minimal calcification to avoid partial volume averaging artifacts from calcified aortic valves.

X-ray angiography data acquisition. Patients underwent diagnostic coronary angiography with simultaneous assessment of the angiographic root plane deemed optimal for eventual TAVI procedure. The angiographic operator was not blinded to the MDCT data at the time of the angiography and sometimes used this data as a start point to assess the optimal angulation of the root angiogram. However, the eventual choice was based on standard angiographic assessment during repeated root injections. A pigtail catheter was placed typically in the noncoronary cusp of the aortic root. The X-ray gantry was angulated to LAO 40, and cranial angulation was gradually added, observing the pigtail catheter and location of calcification at the coronary sinuses. An attempt was made to align the bottom noncoronary sinus (as confirmed by the pigtail catheter) to the bottom of the right and left coronary sinus (as confirmed by sinus calcification) (Fig. 1). The pigtail catheter was selectively manipulated in the right or the left sinus if there were any doubts regarding the nadir of the coronary cusps. Diluted contrast agent (50% Visipaque [GE Healthcare, Princeton, New Jersey] and
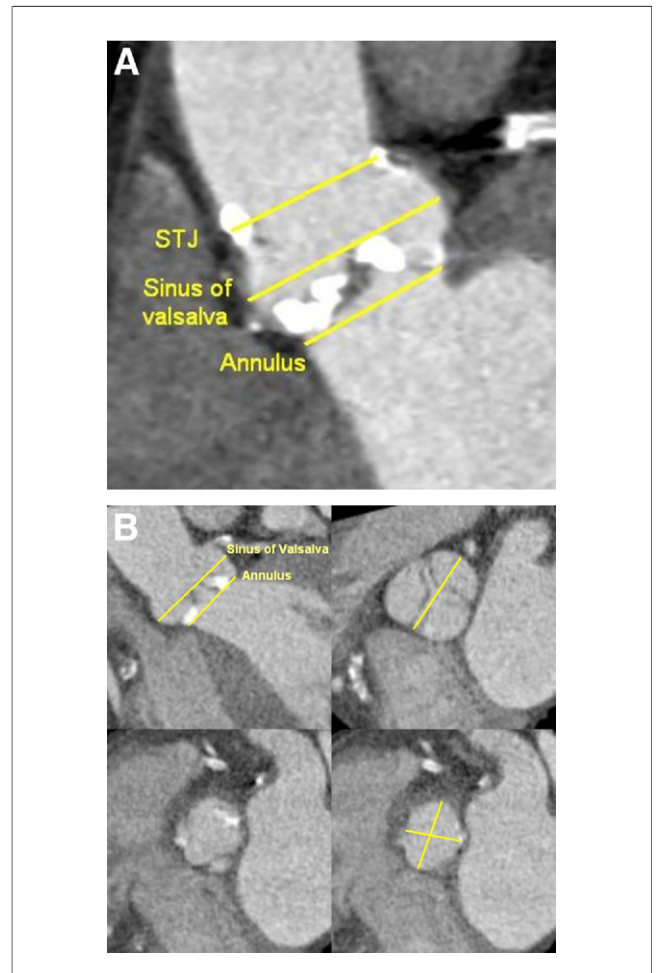
Figure 4. Diameter Measurements in the Aortic Root

Standard diameter measurements in the aortic root. **(A)** A sagittal section of the root and the level of the annulus, sinus of Valsalva, and sinotubular junction (STJ) are shown. **(B)** Measurements in cross-sectional images at the sinus of Valsalva **(upper right)** and annulus **(lower right)** are demonstrated. A cross-section just above the annulus with parts of the 3 leaflets is shown **(lower left)**.

50% saline) was used at 20 cc/s for 0.5 s to deliver a total of 10-cc volume. Most studies were done using biplane equipment with the second gantry angulated to an RAO view. The cranial/caudal angulation was increased or decreased to avoid overlap with the spine or the descending aorta.

X-ray angiography data analysis. Using standard methodology, the measurement tool was calibrated to the respective diagnostic catheter for the aortic root measurements. Using the calibrated measurement tool, the annulus was measured at the lowest hinge point of the aortic valve leaflet (Fig. 5), the sinus of Valsalva at the largest diameter of the bulging sinuses, and the sinotubular junction at the junction of the sinuses and tubular portion of the ascending aorta.

Statistical analysis. All statistics were performed using SPSS software (SPSS Inc., Chicago, Illinois). The mean, standard deviation, and variance of variables were calcu-

Figure 5. Corresponding Angiographic Computed Tomography Images

Examples of corresponding X-ray angiographic and multidetector row computed tomography images of the aortic root in the LAO and RAO projections. Abbreviations as in Figure 3.

Table 1. Baseline Characteristics

	Patients With Severe AS (n = 40)
Age, yrs	80 ± 7
Men	52% (21)
BMI, kg/m^2	28.6 ± 6.1
Creatinine, mg/dl	1.2 ± 0.6
Smoking history	65% (26)
Pulmonary hypertension	25% (10)
Hypertension	75% (30)
Diabetes	58% (23)
Dyslipidemia	53% (21)
History of CAD	70% (28)
History of MI	15% (6)
Peripheral vascular disease	10% (4)
CVA	13% (5)
Endocarditis	3% (1)
COPD	38% (15)
History of CABG	55% (22)
Euroscore	21 ± 16
LVEF	50 ± 11
Peak/mean gradient	82 ± 30/48 ± 19
Aortic valve area	0.6 ± 0.1

Values are mean ± SD or % (n).

AS = aortic stenosis; BMI = body mass index; CABG = coronary artery bypass graft; CAD = coronary artery disease; COPD = chronic obstructive pulmonary disease; CVA = cardiovascular accident; LVEF = left ventricular ejection fraction; MI = myocardial infarction.

lated. Paired *t* tests were used to compare means of variables between contrast-enhanced MDCT and X-ray angiography. The difference between variables was considered statistically significant if the p value was <0.05. The 95% confidence interval (CI) of the difference between the means of variables was calculated. Baseline demographics were recorded as mean ± SD for continuous variables and percentage for categorical variables.

Results

Patient population. Forty patients with severe aortic stenosis (52% female; age 80 ± 7 years) were included in the final analysis. Other clinical and echocardiography variables are shown in Table 1. All patients had trileaflet aortic valves.
X-ray angiography. PLANE ORIENTATION. A suitable root angiogram in the LAO and RAO projections was available in 38 and 40 patients, respectively. For the 38 root angiograms in the LAO projection, the mean LAO angulation was 39 ± 8 (range 15 to 55) and mean cranial angulation 25 ± 7 (range 4 to 40). For the 40 root angiograms in the RAO projection, the mean RAO angulation was 25 ± 5 (range 12 to 37) and mean caudal angulation 21 ± 9 (range 0 to 40).

ANNULUS MEASUREMENTS. X-ray angiographic diameter measurements of the aortic annulus, sinus of Valsalva, and sinotubular junction in the LAO and RAO projections are shown in Table 2. The annulus measurement in the LAO

and RAO root angiograms (2.3 ± 0.4 cm and 2.3 ± 0.3 cm, respectively) was not significantly different (p = 0.67).
Contrast-enhanced MDCT. PLANE ORIENTATION. The cranial angulation for the standard LAO 40 projection was 24 ± 9 (n = 40; range 1 to 40). For the MDCT image corresponding to the LAO root X-ray angiogram (LAO 39), the cranial angulation was 23 ± 8 (n = 38; range 5 to 37). There was no significant difference between the 2 cranial angulations (p = 0.5; 95% CI: −2 to 1).

The caudal angulation for the standard RAO 20 projection was 27 ± 10 (n = 40; range 11 to 66). For the CT image corresponding to the angiographic RAO X-ray root angiogram (RAO 25), the caudal angulation was 29 ± 10 (n = 40; range 13 to 66). There was a small but significant difference between the 2 caudal projections (p ≤ 0.0001; 95% CI: 1 to 3).

Table 2. Angiographic Diameter of the Aortic Annulus, Sinus of Valsalva, and STJ in LAO and RAO Root Angiograms

	LAO (n = 38)	RAO (n = 40)	p Value (95% CI*)
Annulus, cm	2.3 ± 0.4	2.3 ± 0.3	0.67 (−0.07 to 0.1)
Sinus of Valsalva, cm	3.5 ± 0.6	3.4 ± 0.5	0.3 (−0.07 to 0.2)
STJ, cm	2.9 ± 0.6	2.8 ± 0.4	0.3 (−0.05 to 0.2)

Data obtained using paired *t* test. *Describes the 95% confidence interval (CI) of the difference between the means of variables.

LAO = left anterior oblique; RAO = right anterior oblique; STJ = sinotubular junction.

ANNULUS MEASUREMENTS. In the reformatted cross-sectional MDCT image of the aortic annulus, the mean minimal and maximal diameters were 2.1 ± 0.23 cm and 2.5 ± 0.19 cm, respectively. The average diameter was 2.3 ± 0.2 cm.

In the reformatted oblique sagittal MDCT images of the root matched to the angulation of the X-ray root angiograms, the diameter of the annulus was 2.4 ± 0.3 cm in the LAO 39 and 2.2 ± 0.3 cm in the RAO 25 projection. The difference between the LAO and RAO measurements was significant (p = 0.018) (Table 3).

Comparison between X-ray angiography and contrast-enhanced MDCT. PLANE ORIENTATION. The cranial angulation for the root X-ray angiogram in the LAO projection (mean LAO: 39 ± 8, n = 38) and the matched MDCT image were not significantly different (cranial: 25 ± 7 vs. 23 ± 8; p = 0.214; 95% CI: −5 to 1). There was also no significant difference between the root angiogram and the standard LAO 40 MDCT image (cranial: 25 ± 7 vs. 23 ± 10; p = 0.3; 95% CI: −2 to 5).

The caudal angulation for the root angiogram in the RAO projection (mean RAO: 25 ± 5, n = 40) and the matched CT reconstruction were significantly different (caudal: 21 ± 9 vs. 29 ± 10; p = 0.002; 95% CI: 3 to 12). There was also a significant difference between the root angiogram and the standard MDCT image (caudal: 21 ± 9 vs. 27 ± 10; p = 0.02; 95% CI: 1 to 10).

ANNULUS MEASUREMENTS. The X-ray angiographic annulus diameter, in the LAO projection was not significantly different from the MDCT diameter in the same LAO projection (2.3 ± 0.3 cm vs. 2.4 ± 0.3 cm; p = 0.052; 95% CI: −0.1 to 0.2) (Table 4).

There was a small but significant difference between the X-ray angiographic annulus diameter in the RAO projection and the MDCT diameter in the same RAO projection (2.4 ± 0.3 cm vs. 2.2 ± 0.3 cm; p = 0.029; 95% CI: −0.2 to −0.01) (Table 4).

The mean X-ray angiographic annulus diameter (combining LAO and RAO measurements) was not significantly different from the mean cross-sectional MDCT diameter (combining minimal and maximal diameters) (2.3 ± 0.4 cm vs. 2.3 ± 0.3 cm, p = 1.0; 95% CI: −0.15 to 0.15).

Table 3. MDCT-Derived Diameter of Aortic Annulus, Sinus of Valsalva, and STJ in Reformatted LAO and RAO Planes, Matched to Angiography

	LAO (n = 38)	RAO (n = 40)	p Value (95% CI*)
Annulus, cm	2.4 ± 0.3	2.2 ± 0.3	0.018 (0.01 to 0.2)
Sinus of Valsalva, cm	3.3 ± 0.3	3.2 ± 0.4	0.01 (0.02 to 0.2)
STJ, cm	2.5 ± 0.3	2.5 ± 0.3	0.55 (−0.06 to 0.1)

Data obtained using paired *t* test. *Describes the 95% CI of the difference between the means of variables.

MDCT = multidetector row computed tomography; other abbreviations as in Table 2.

Table 4. Comparison of Annulus, Sinus of Valsalva, and STJ Dimensions in Matched LAO/Cranial and RAO/Caudal Planes Between X-Ray and MDCT Angiography

|	LAO CT	LAO Angiography	p Value (95% CI*)
Annulus, cm	2.4 ± 0.3	2.3 ± 0.3	0.052 (−0.1 to 0.2)
Sinus of Valsalva, cm	3.3 ± 0.3	3.5 ± 0.6	0.04 (−0.4 to 0.1)
STJ, cm	2.5 ± 0.3	2.8 ± 0.5	<0.0001 (−0.5 to 0.1)
	RAO CT	RAO Angiography	
Annulus, cm	2.2 ± 0.3	2.4 ± 0.3	0.029 (−0.2 to 0.01)
Sinus of Valsalva, cm	3.2 ± 0.4	3.4 ± 0.5	0.01 (−0.3 to 0.04)
STJ, cm	2.5 ± 0.3	2.8 ± 0.4	<0.0001 (−0.4 to 0.1)

Data obtained using paired *t* test. *Describes the 95% CI of the difference between the means of variables.

Abbreviations as in Tables 2 and 3.

Discussion

Comparing the angulation of the aortic root in conventional X-ray angiograms and reformatted MDCT images, we found good agreement in the LAO projections and small but significant differences in the RAO projections. Diameter measurements with MDCT at the annulus demonstrated an oval shape with good agreement between the mean MDCT and mean X-ray angiographic diameters.

Recent MDCT studies have compared annulus and root diameter measurements among MDCT, echocardiography, and angiography (3–7,11). Consistently, these reports demonstrated an oval shape of the annulus and moderate correlation of MDCT with echocardiography and X-ray angiography. These data are important in the context of TAVI, because planning of the procedure is dependent on the assessment of detailed internal measurements of the aortic root (1,2). However, there is also a need to understand the orientation of the root relative to the body axis. The assessment of root orientation is critical for precise positioning of the stent/valve along the centerline of the aorta and perpendicular to the valve plane. The current standard approach is based on the identification of X-ray root angiograms in 1 or preferably 2 orthogonal planes before the procedure after repeated root injections. Our data demonstrates that a preprocedural MDCT angiography of the aortic root allows prediction of the angulation of the root angiogram, which could facilitate the angiographic procedure and reduce the number of root injections (Fig. 2). The potential advantage of MDCT is the 3D nature of the image dataset, which after fast acquisition allows off-line reformations along unrestricted planes.

In our study, the final root angiogram was selected close to the LAO 40 and RAO 20 projections. In particular, the MDCT reformat in the LAO 40 projec-
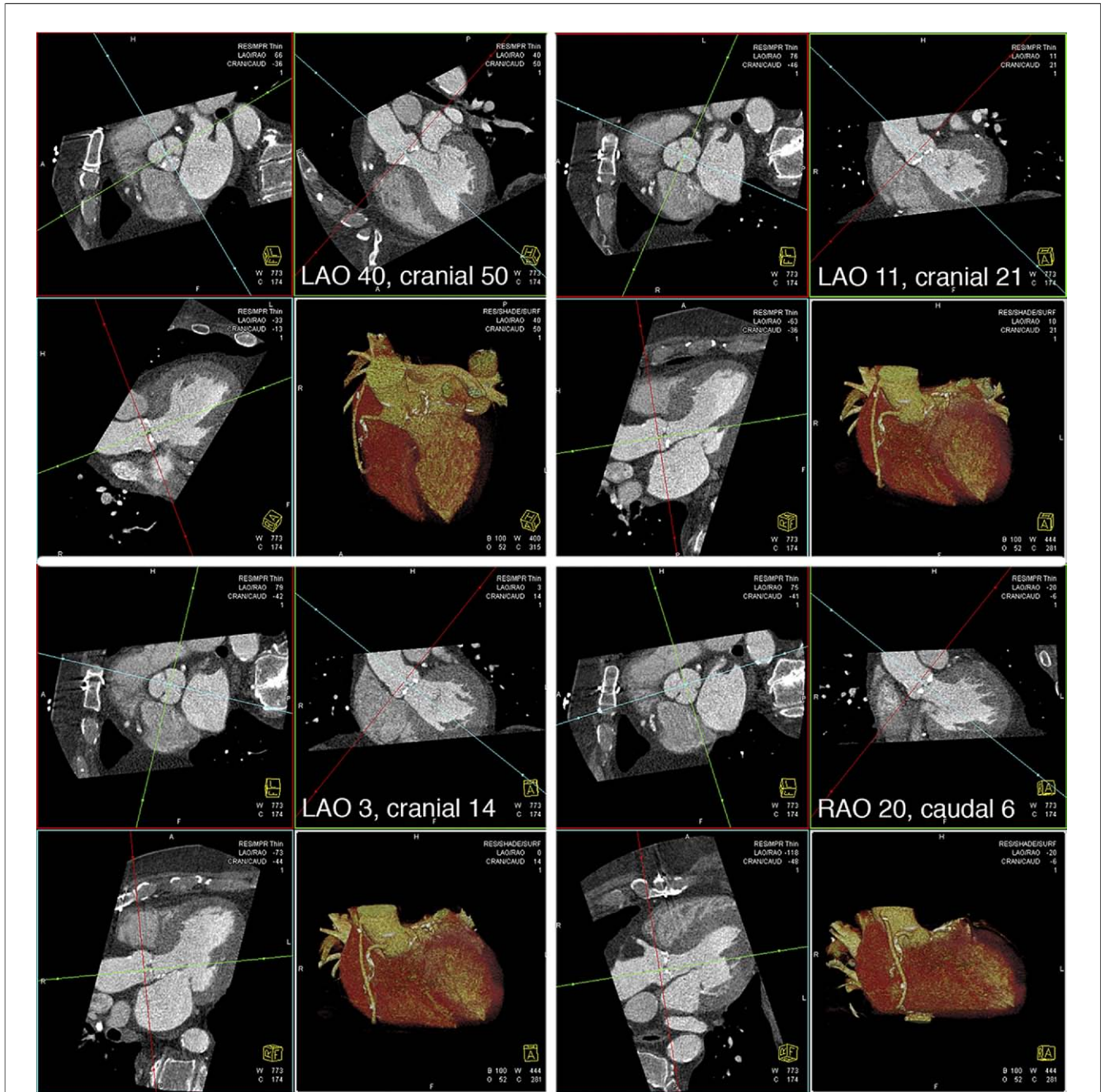
Figure 6. Identification of Projections Achievable in the Catheterization Laboratory

In this patient, the LAO 40 angulation is associated with a very steep cranial angulation (cranial 50), which would be impractical in the catheterization laboratory. Additional multidetector row computed tomography planes at different LAO angulations showed a more appropriate shallow cranial angulation (e.g., cranial 14 at an LAO 3 angulation). CRAN/CAUD = cranial/caudal; MPR = multiplanar reconstruction; other abbreviations as in Figure 3.

tion was a good approximation for the final X-ray root angiogram (Fig. 3) and can therefore be used as a starting point for the angiographic identification of the optimal root angiogram, during the interventional procedure. However, depending on the orientation of the root, the LAO 40 view is occasionally associated with a steep cranial angulation, which would be impractical in the catheterization laboratory (Fig. 6). In these patients, we recommend reformation of multiple MDCT planes at different LAO angulations, with the goal of identifying a plane with an associated cranial angulation <20 to 25 as a starting point (Fig. 6).

Providing multiple planes is also important, because the choice of the X-ray angiographic plane is dependent on the feasibility of these angles in the catheterization laboratory and the ability to separate the root from the surrounding structures. In this context, it is critical to understand that the aortic valve plane can be interrogated in any RAO and LAO angulation if the corresponding cranial or caudal angulation is added.

The 3D nature of the MDCT image sets allows unlimited reformations of potential angiographic planes for any LAO/RAO angulation, and advanced analysis could predict overlap of the spine or aorta. Conceivably, mathematical modeling based on 2 standard reformations (e.g., LAO 40 and RAO 20) should allow determination of the cranial/caudal angulation for any intermediate LAO/RAO angulations. Such data, correlating 3D MDCT data with 2-dimensional, planar angiographic projections are of increasing interest beyond TAVI. For example, rotational C-arm angiography has the potential to provide tomographic as well as planar images, as was recently described in electrophysiology and neurointervention (12–15). Eventually these concepts will need to be examined in well-designed prospective trials not only examining feasibility but also clinical influence, including reduction of contrast agent use and radiation exposure.

Based on the emerging data, our group currently uses the following approach for CT imaging. 1) Following current clinical recommendations, sizing of the annulus for inclusion/exclusion and choice of device size are based on echocardiographic measurements. However, if available, the CT assessment of the annulus size are also taken into consideration. Thin-sliced, gated, contrast-enhanced CT studies typically demonstrated a more oval shape of the annulus, and the mean diameter is most comparable to the echocardiographic measurements. If there is a large discrepancy in the transthoracic echocardiography and CT measurements, transesophageal echocardiography is performed to better understand annulus size. 2) Whereas thin-sliced, gated, contrast-enhanced CT studies allow detailed evaluation of the anatomy of the aortic root (size, geometry, and calcification of the leaflets and root and location of the coronary ostia), these data are routinely obtained from pre-operative and intraoperative echocardiography and angiography. If extensive sinotubular calcification is suspected, this is further evaluated with CT in order to understand potential restrictions to balloon expansion at the time of valve replacement. 3) The angulation of the valve plane as described in the current report is evaluated based on review of available CT scans (note that these measurements are possible in noncontrast-enhanced scans and chest CT performed for unrelated indications). 4) Planning of peripheral access is based on CT scans of the aorta and iliac arteries and limited angiograms performed at the time of pre-procedural catheterization. 5) In patients with significant renal impairment, CT of the ileo-femoral arteries are performed by intra-arterial injection of about 15 ml of contrast agent via a pigtail catheter placed below the renal arteries. If this is not feasible, noncontrast-enhanced studies provide information about calcification and angulation. 6) In individual patients, the need for CT is weighted against associated contrast administration and radiation exposure.

Study limitations. The reason for the discrepancy between X-ray angiography and MDCT, in particular in the RAO angulations, likely stems in part from the fact that X-ray angiographic assessment requires preventing overlap of the aortic root with the spine and descending aorta. Also patient positioning during the MDCT and angiographic procedure is similar but may not be identical without further standardization.

The angiographic operator was aware of the MDCT measurements in the standard LAO 40 and RAO 20 projections at the time of the diagnostic X-ray angiogram. Whereas this may have influenced the initial angulation of the C-arm, the choice of the final root angiogram was based on routine angiographic procedure as described in this report.

In the vast majority of patients, and all patients in this study, the LAO projection is associated with cranial angulation, and the RAO projection with caudal angulation. Because averaging between LAO and RAO or cranial and caudal angulations is not possible without further mathematical modeling, we separated the LAO and RAO data.

The MDCT protocol used for root imaging is associated with contrast administration and significant radiation exposure. Reducing the amount of contrast is critical in the elderly patient population with high prevalence of reduced renal function, which is currently considered for TAVI. We have recently used standard electrocardiogram-gated MDCT acquisitions (prospectively triggered or retrospectively gated) of the chest/aorta without contrast administration. In our experience, assessment of the angiographic planes is not limited in these acquisitions.

Although our data demonstrate the feasibility of predicting the appropriate angiographic plane, we did not evaluate procedural success and clinical outcome in comparison to standard angiographic approaches. Therefore, the data do not allow assessment of clinical utility.

Conclusions

In summary, 3D MDCT image sets allow detailed insights into the complex anatomy of the aortic root including root orientation. Such data may improve the planning process for novel, transcatheter approaches to valve disease. Whereas MDCT provides detailed data, the impact on clinical decision making in the context of TAVI warrants further

investigation to define the eventual role of these imaging modalities.

Reprint requests and correspondence: Dr. Paul Schoenhagen, Imaging Institute and Heart and Vascular Institute, Cleveland Clinic, 9500 Euclid Avenue, Desk J1-4, Cleveland, Ohio 44195. E-mail: schoenp1@ccf.org.

REFERENCES

1. Vahanian A, Alfieri O, Al-Attar N, et al., on behalf of European Association of Cardio-Thoracic Surgery; European Society of Cardiology, European Association of Percutaneous Cardiovascular Interventions. Transcatheter valve implantation for patients with aortic stenosis: a position statement from the European Association of Cardio-Thoracic Surgery (EACTS) and the European Society of Cardiology (ESC), in collaboration with the European Association of Percutaneous Cardiovascular Interventions (EAPCI). Eur Heart J 2008;29:1463–70.
2. Schoenhagen P, Tuzcu EM, Kapadia SR, et al. Three-dimensional imaging of the aortic valve and aortic root with computed tomography: new standards in an era of transcatheter valve repair/implantation. Eur Heart J. 2009;30:2079–86.
3. Tops LF, Wood DA, Delgado V, et al. Noninvasive evaluation of the aortic root with multislice computed tomography: implications for transcatheter aortic valve replacement. J Am Coll Cardiol Img 2008; 1:321–30.
4. Knight J, Kurtcuoglu V, Muffly K, et al. Ex vivo and in vivo coronary ostial locations in humans. Surg Radiol Anat 2009;31:597–604.
5. Akhtar M, Tuzcu EM, Kapadia SR, et al. Aortic root morphology in patients undergoing percutaneous aortic valve replacement. Evidence of aortic root remodeling. J Thorac Cardiovasc Surg 2009;137:950–6.
6. Stolzmann P, Knight J, Desbiolles L, et al. Remodelling of the aortic root in severe tricuspid aortic stenosis: implications for transcatheter aortic valve implantation. Eur Radiol 2009;19:1316–23.
7. Wood DA, Tops LF, Mayo JR, et al. Role of multislice computed tomography in transcatheter aortic valve replacement. Am J Cardiol 2009;103:1295–301.
8. Kurra V, Schoenhagen P, Roselli EE, et al. Prevalence of significant peripheral artery disease in patients evaluated for percutaneous aortic valve insertion: preprocedural assessment with multidetector computed tomography. J Thorac Cardiovasc Surg 2009;137:1258–64.
9. Kapadia SR, Goel SS, Svensson L, et al. Characterization and outcome of patients with severe symptomatic aortic stenosis referred for percutaneous aortic valve replacement. J Thorac Cardiovasc Surg 2009;137: 1430–5.
10. Cademartiri F, Nieman K, van der Lugt A, et al. Intravenous contrast material administration at 16-detector row helical CT coronary angiography: test bolus versus bolus-tracking technique. Radiology 2004;233: 817–23.
11. Laissy JP, Messika-Zeitoun D, Serfaty JM, et al. Comprehensive evaluation of preoperative patients with aortic valve stenosis: usefulness of cardiac multidetector computed tomography. Heart 2007;93: 1121–5.
12. Nölker G, Gutleben KJ, Marschang H, et al. Three-dimensional left atrial and esophagus reconstruction using cardiac C-arm computed tomography with image integration into fluoroscopic views for ablation of atrial fibrillation: accuracy of a novel modality in comparison with multislice computed tomography. Heart Rhythm 2008;5:1651–7.
13. Knackstedt C, Mühlenbruch G, Mischke K, et al. Imaging of the coronary venous system: validation of three-dimensional rotational venous angiography against dual-source computed tomography. Cardiovasc Intervent Radiol 2008;31:1150–8.
14. Dörfler A, Struffert T, Engelhorn T, Richter G. Rotational flat-panel computed tomography in diagnostic and interventional neuroradiology. Rofo 2008;180:891–8.
15. Kyriakou Y, Richter G, Dörfler A, Kalender WA. Neuroradiologic applications with routine C-arm flat panel detector CT: evaluation of patient dose measurements. AJNR Am J Neuroradiol 2008;29:1930–6.

Key Words: multidetector computed tomography ■ angiography ■ transcatheter aortic valve implantation ■ aortic stenosis ■ aortic valve.